Proceedings of the Federated Conference on
Computer Science and Information Systems pp. 701–708

DOI: 10.15439/2015F159
ACSIS, Vol. 5

# DCT trigger for a detection of very inclined showers in the Pierre Auger surface detector Engineering Array in the new High-Resolution Front-End based on the Cyclone V FPGA

Zbigniew Szadkowski
University of Łódź
Department of Physics and Applied Informatics
Faculty of High-Energy Astrophysics
90-236 Łódź, Pomorska 149
e-mail : zszadkow@kfd2.phys.uni.lodz.pl

***Abstract*—The paper presents the first results from the trigger based on the Discrete Cosine Transform (DCT) operating in the new Front-End Boards with Cyclone V FPGA deployed in 8 test surface detectors in the Pierre Auger Engineering Array.**

**The patterns of the Analog-to-Digial Converter (ADC) traces generated by very inclined showers were obtained from the Auger database and from the CORSIKA simulation package supported next by OffLine reconstruction Auger platform which gives a predicted digitized signal profiles. Simulations for many variants of the initial angle of shower, initialization depth in the atmosphere, type of particle and its initial energy gave a boundary of the DCT coefficients used next for the on-line pattern recognition in the FPGA.**

**Preliminary results have proven a right approach. We registered several showers triggered by the DCT for 120 MSps and 160 MSps.**

## I. Introduction

THE AIM of the Pierre Auger Observatory [1] is measuring of cosmic rays at the ultra-high energy with sufficient statistics and resolution. 1680 water Cherenkov surface detectors (SD) are distributed over an area of 3000 km$^2$ for measuring the charged particles associated with extensive air showers (EAS) and 24 telescopes with $30 \times 30$ degrees of field of view and 12 m$^2$ mirror area each to observe the fluorescent light produced by charged particles in the EAS during operation on clear moonless nights. The simultaneous observation of EAS by the ground array and the fluorescent light known as a "hybrid" event [2] [3] improves the resolution of the reconstruction considerably and, thanks to the calorimetric nature of the fluorescent light emitted, provides energy measurements virtually independent of hadronic interaction models. Each SD station is equipped in three 9-inch photomultiplier tubes (PMTs) reading out the Cherenkov light from the 12 $m^3$ of purified water contained in each tank. Two independent trigger modes are implemented in the SD to detect, in a complementary way, the electromagnetic and muonic components of an air-shower [4]. The first mode is a simple threshold trigger, which requires the coincidence of the three PMTs each above 1.75 $I_{VEM}^{peak}$. This trigger is used to select large signals that are not necessarily spread in time. The second mode takes into account that, for other than very inclined showers or signals from more vertical showers very close to the shower axis, the arrival of particles and photons at the detector is dispersed in time, at least 13 bins in 120 time bins of a sliding window of 3 $\mu$s are required to be above a threshold of 0.2 $I_{VEM}^{peak}$ in coincidence in two of any 3 PMTs.

Very inclined showers generated by hadrons and starting their development early in the atmosphere produce a relatively thin muon pancake ($\sim$1m thickness) on a detection level. Ultra-relativistic charged particles trespassing the water in a surface detector generate the Cherenkov light detected next in photo-multipliers (PMT). A direct light gives a peak with a very short rise time and fast exponential attenuation. The DCT trigger allows recognition of ADC traces with specific shapes The standard trigger requires 3-fold coincidences in a single time bin. The present sampling frequency in the surface detectors is 40 MHz. The new Front-End Board developed for the Auger-Beyond-2015 surface detector upgrade allows a sampling up to 250 MSps (120 MSps and 160 MSps were used in tests).

Neutrinos can generate showers starting their development deeply in the atmosphere, known as "young" [5] [6]. They contain a significant amount of an electromagnetic component, usually preceded by a muon bump. Simulations show [7] that it is often fully separated from the electromagnetic fraction and the 16-point DCT algorithm can also be used..

A probability of 3-fold coincidences of direct light corresponding to a standard Auger trigger is relatively low. Much more probable are 2-fold coincidences of a direct light. The 3rd PMT is next hit by reflected light, but with some delay. By fast sampling (120-160 MSps) this delay gives signal in the next time bins. The standard T1 trigger ceases giving a sufficient rate for horizontal and very inclined showers. The rate drops down below an acceptable level. We had to modify the T1 trigger to get approximately standard trigger rate.

978-83-60810-66-8/$25.00

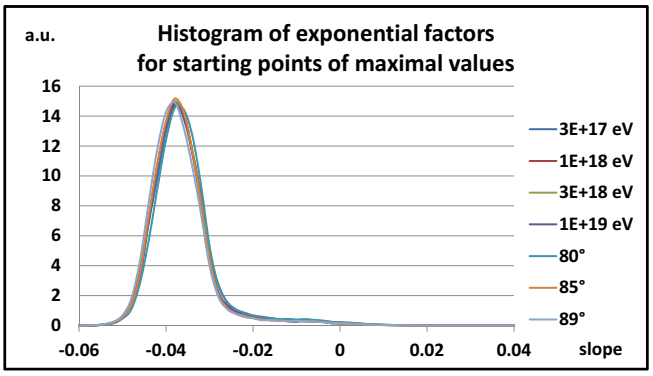


Fig. 1. Histogram of exponential factors for traces starting from the maximal values.

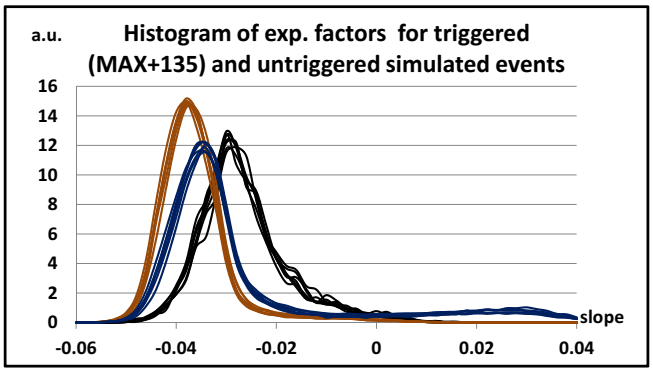


Fig. 2. Histogram of exponential factors for triggered traces starting from the maximal values (as in Fig. 1 - red), from the standard T1 threshold = 1.75 VEM (135 ADC-units)(blue) and for non-triggered (black) events.

Cherenkov light generated by very inclined showers crossing the Auger tank can reach the PMT directly without reflections on Tyvec® liners (a special material with 95% of reflectivity). Especially for "old" showers the muonic front is very flat. This together corresponds to very short direct light pulse falling on the PMT and in consequence very short rise time of the PMT response. For vertical or weakly inclined showers, where the geometry does not allow reaching the Cherenkov light directly on the PMT, the light pulse is collected from many reflections on the tank walls. Additionally, showers developing for not so high slant depth are relatively thick. These give a signal from a PMT as spread in time and relatively slow increasing. A very short rise time together with a relatively fast attenuated tail could be a signature of very inclined showers. We observe numerous very inclined showers crossing the full array but which "fire" only few surface detectors. For that showers much more tanks should have been hit. Muonic front produces PMT signals either too low for 3-fold coincidences or desynchronized in time. This may be a reason of "gaps" in the array of activated tanks.

Two-fold coincidences of DCT coefficients allow triggering signals currently being ignored due to either too high amplitude threshold or due to their de-synchronization in time causing a tank geometry. Three DCT engines implemented into Cyclone® V E 5CEFA9F31I7N FPGA used ∼60% of DSP blocks generate the spectral trigger, when in at least 2 channels 8 DCT coefficients simultaneously are inside the acceptance lane. Additional veto signal (analyzing the amplitude) controls a trigger rate to avoid a saturation of a transmission channel. Both lab and long-term field measurements on the test tank confirm a high efficiency of the recognition of expected patterns of ADC traces.

Auger data (40 MSps) show that hadron induced showers with dominant muon component (investigated in a zenith angle of $70-90°$) give an early peak with a typical rise time mostly from 1 to 2 time bins and exponentially attenuated tail. Very inclined showers with well defined shape can be detected by a pattern recognition technique, in particular by a spectral trigger based on the Discrete Cosine Transform [8] [9] [10] [11]. The DCT trigger cannot be implemented into currently used Front-End Boards with ACEX® [12] and Cyclone® [13] FPGAs due to a lack of DSP blocks. New Front-End Board with Cyclone® V E FPGA successfully passed tests on the field collecting Auger data even with 160 MHz sampling [9]. The DCT trigger was tested with 120 and 160 MHz. Scaled to the 1st harmonics DCT coefficients are independent of the amplitude. They are determined by the shape only. This causes that the DCT trigger could also be accidentally generated by very low noise pulses with the required characteristics. In order to cut this type of the spurious triggers, the spectral trigger was also supported by the "veto" amplitude threshold of ∼20 ADC-counts. Pulses above this threshold are analyzed next with the DCT engines.

Due to noise and other factors which can distort the shape of the PMT pulse, strict conditions imposed on all coefficients are too strong. The DCT trigger has been generated if a subset of DCT coefficients (similar to the Occupancy in the ToT) has been simultaneously "fired". Simulations performed for various artificial level of additional noise (0 - 6 ADC-counts) showed that even a significant noise contribution does not violate an efficiency of the DCT trigger. A little bit higher noise in Cyclone® V E Front-End in comparison to a noise level in the previous FEB generations with 40 MHz sampling should not be a significant factor. The new 160 MHz sampling Cyclone® V E Front-End Boards are not equipped in the anti-aliasing filters. This keeps a flexibility for various possible sampling frequencies, however, registered shape is not smoothed and provides even very short one time-bin peaks (6.25 ns) corresponding to reflections from Tyvec walls. Such a very precisely reconstruction of timing in the ADC traces violates in some sense a fundamental assumption on a smooth exponential attenuation of the tail. We had to introduce some corrections to take into account also this effect. The CORSIKA and OffLine simulations do not show that the reflections may significantly reduce an efficiency of this approach. However, the Auger simulation/reconstruction packages assume 60 MHz cut-off Nyquist filter, which in real Cyclone® V E Front-End has not been introduced. Thus, the simulations (available only for the "official" 120 MHz sampling frequency) give rather hints for higher 160 MSps sampling and real DCT

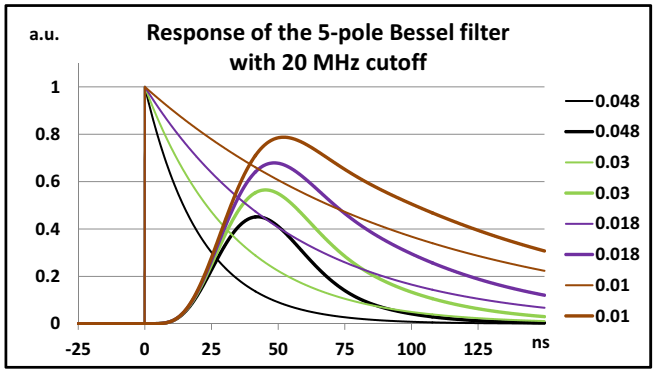


Fig. 3. Pulses as a response on a unity jump with an exponential attenuation with the factors $\alpha$ = 0.048, 0.03, 0.018 and 0.01, respectively.

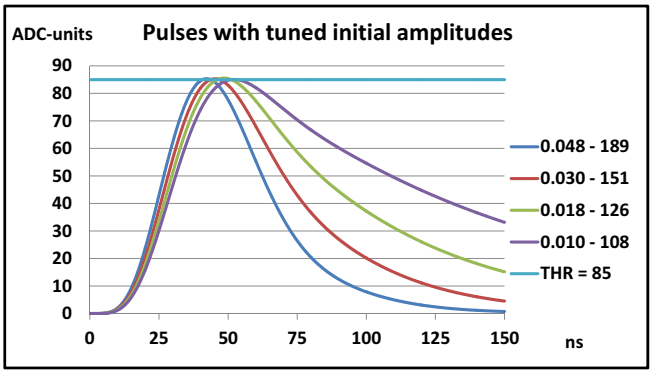


Fig. 4. Pulses filtered by the 5-pole Bessel filter with 20 MHz cutoff with amplitudes: 189, 151, 126 and 108 ADC-units, respectively for 0.048, 0.03, 0.18 and 0.01 exponential factors.

trigger implementation required several step by step optimizations.

## II. CORSIKA AND OFFLINE SIMULATIONS

We simulated the surface detector response on proton induced showers for energy $3 * 10^{17}$ eV, $10^{18}$ eV, $3 * 10^{18}$ eV and $10^{19}$ eV and for angles 80°, 85° and 89°. The initial points were selected for 2, 3, 4, 5 and 10 $kg/cm^2$, if the angle allowed on this geometrical configuration. ADC traces were collected as triggered (3-fold coincidences in a single time bin) and non-triggered (the standard T1 trigger condition not obeyed, traces registered in neighboring detectors). The standard T1 threshold 1.75 VEM was set in simulations.

Data from standard 40 MHz sampling simulation was used for an optimization of the condition of the DCT trigger for 120 and 160 MSps. Data for 16-point DCT trigger for 160 and 120 MSps corresponds to 100 and 133 ns of ADC trace, respectively. These intervals correspond to 4 and 5 time bins for the standard 40 MSps sampling. As expected proton induced showers generate ADC traces with rapid jump from a pedestal level with relative fast exponentially attenuated tails. We investigated exponential factors of traces in the interval of 125 ns (5 time-bins) selecting parts of traces starting from

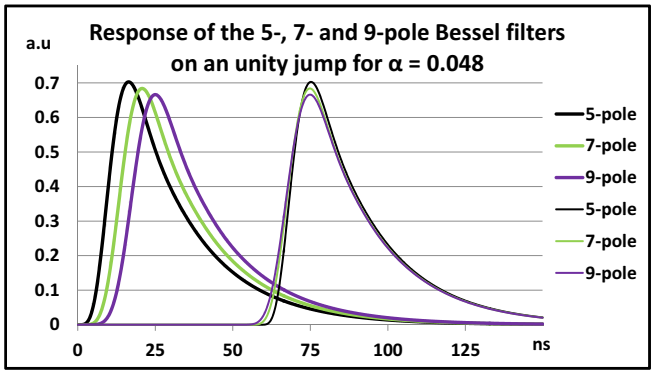


Fig. 5. Response on an unity jump of Bessel filters with 5,7,and 9 poles, respectively. The left curves show response on a jump for 0 ns. The right curves are adjusted to get maximum in the same time bin.

the maximum value (MAX for triggered (Fig. 1) and non-triggered) and from the standard threshold level (135 ADC-units for triggered only). According to Fig. 2 we see that ranges of exponential factors depend on amplitudes of signals. Traces investigated from the maximum values (variant A)(red curves on Fig. 2) shows faster attenuation than investigating from the T1 threshold level (variant B). Non-triggered traces (with amplitudes lower than T1 threshold level at least in one channel) show much slower attenuation (variant C). For we get the following ranges for attenuation factors $\alpha$ in the function ADC = exp(-$\alpha$*t), where t in nanoseconds.

- variant A : 0.048 - 0.030 : ∼89-90% of traces
- variant B : 0.048 - 0.010 : ∼83-86% of traces
- variant C : 0.042 - 0.014 : ∼89-91% of traces

The variant B gives the worst estimation, however, it is not unexpected, as traces may still rise after crossing the T1 threshold. This variant is presented to show the dependence of the exponential factor on the amplitude of signal.

## III. 5-POLE BESSEL FILTER WITH 20 MHZ CUTOFF

According to the Nyquist theorem digitized ADC data should be filtered by the anti-aliasing filter before their processing. For the 40 MSps sampling the cutoff of the filter is 20 MHz. The ACEX® and Cyclone® FEBs were equipped in 5-pole Bessel filters. The Bessel filter provides a maximally flat group/phase delay (maximally linear phase response), which preserves the wave shape of filtered signals in the passband. Higher order of the filter gives steeper frequency characteristic for stop-band, however it requires more sophisticated filter circuit with relatively low values of capacitors. The parasitic PCB capacity became no negligible factor. The transfer function H(s) for the 5-pole Bessel filter with 20 MHz cutoff is as follows:

$$H(s) = \frac{K}{(s-p)(s-z_1)(s-z_1^*)(s-z_2)(s-z_2^*)} \quad (1)$$

where $K = 3.1336e + 40$, $p = -0.11642e9$, $z_1 = -0.07421e9 + 0.114e9 * j$, $z_2 = -0.10701e9 + 0.005563e9 * j$.

Let us calculate the response of the Bessel filter on the unity jump with the exponential attenuation tails with $\alpha$ = 0.048, 0.03, 0.018 and 0.01, respectively. The Laplace transform for the function x(t) = exp(-$\alpha$*t) is X(s) 1/(s+$\alpha$). The factor $\alpha$ is given for time in nanoseconds. The signal response we get with the inverse Laplace transform:

$$y(t) = Y(s)^{-1} = (H(s) * X(s))^{-1} \quad (2)$$

$$\begin{aligned} Y(t) &= (A * sin(z'_{Im,1} * t) + B * cos(z'_{Im,1} * t) * e^{z'_{Re,1} * t} \\ &+ (C * sin(z'_{Im,2} * t) + D * cos(z'_{Im,2} * t) * e^{z'_{Re,2} * t} \\ &+ E * e^{p' * t} + F * e^{-\alpha * t} \end{aligned} \quad (3)$$

where: $p' = p * 10^{-9}$ $z'_{1,2} = z_{1,2} * 10^{-9}$

TABLE I
COEFFICIENTS FOR EQ. 3 , WHERE TIME GIVEN IN NANOSECONDS

| $\alpha$ | A | B | C | D | E | F |
|---|---|---|---|---|---|---|
| 0.048 | 1.1258 | 1.2349 | -10.080 | 3.4118 | -9.7361 | 5.0893 |
| 0.030 | 1.2354 | 1.0147 | -8.1538 | 4.0062 | -7.7082 | 2.6873 |
| 0.018 | 1.2697 | 0.8677 | -7.1206 | 4.1119 | -6.7684 | 1.7888 |
| 0.010 | 1.2778 | 0.7740 | -6.5323 | 4.1101 | -6.2596 | 1.3754 |

Fig. 3 shows responses on an unity jump of the input signal with various exponential attenuation factors. We can see that:

- pulses are delayed on 40 - 50 ns,
- an amplitude of pulses depends on the exponential factor.

A dependence of output signal amplitude on an exponential factor causes that short pulses have to have higher amplitudes to be above the threshold level. Fig. 4 shows pulses with tuned amplitudes to reach at least the T1 threshold level (1.75 VEM ∼85 ADC-units).

Let us notice that for all investigated values of $\alpha$ we get : $\alpha < |z_{Re,1}| < |z_{Re,2}| < |p|$. This causes that the exponential term $e^{-\alpha * t}$ attenuates slower than other terms in Eq. 3and practically it only survives for $t >$∼50 ns (after a maximum). So, the attenuation (exponential) factor for a output tail remains the same as in the input signal with rapid jump and exponential tail.

This means that all estimations of attenuation factors for ADC traces from the shower simulations remains valid and the Bessel filter does not affect the attenuation characteristics after the maximum of pulse. The rise time still depends significantly on an order of the filter and the cutoff frequency.

## IV. BESSEL FILTERS FOR THE SDE UPGRADE

According to golden rules the new Front-End electronics with the sampling frequency of 120 MHz should be equipped in the 60 MHz cutoff anti-aliasing filter. Higher order of the filter provides sharper frequency characteristic in the stop-band, but it introduces slightly bigger suppression and few nanoseconds additional delay (Fig. 5).

Fig. 5 shows that 9-pole filter in comparison to 5-pole one:

- introduces bigger delay,
- suppresses stronger the signal,
- provides the same attenuation factor for tails.

5-pole Bessel filter for the upgrade design seems to be enough. Nevertheless, the test system installed in the Auger Engineering Array is considered to verify various configurations for sampling frequencies, data resolutions, trigger conditions etc. The sampling frequencies determine the cutoff in the anti-aliasing filters. For 120 MSps the cutoff should equals 60 MHz. On the other hand this cutoff would be too low for the 160 MSps. The hardware implementation of the Bessel filter on the PCB is difficult (parasitic capacitors have to be taken into account, a tolerance of components should be better than 1%. For resistors it is no problem, however for capacitors it is. Namely, a dynamic switching of cutoff frequencies in hardware filters is impossible. A requirement of wide spectrum of sampling frequencies excludes any fixed filter to be implemented on the PCB.

For this reason the Front-End has been designed without internal anti-aliasing filter at all.

## V. RISE TIMES OF THE SIGNAL WAVEFORMS

Fig. 5 suggests that a rise time of a unity jump takes at least 2-3 time-bins (20 - 25 ns) for the 120 MSps. This is fully confirmed by the CORSIKA + Offline simulations. Fig. 6a shows a contribution of signals waveforms with 1-, 2- and more time bins, respectively. The contribution of 1-time-bin is

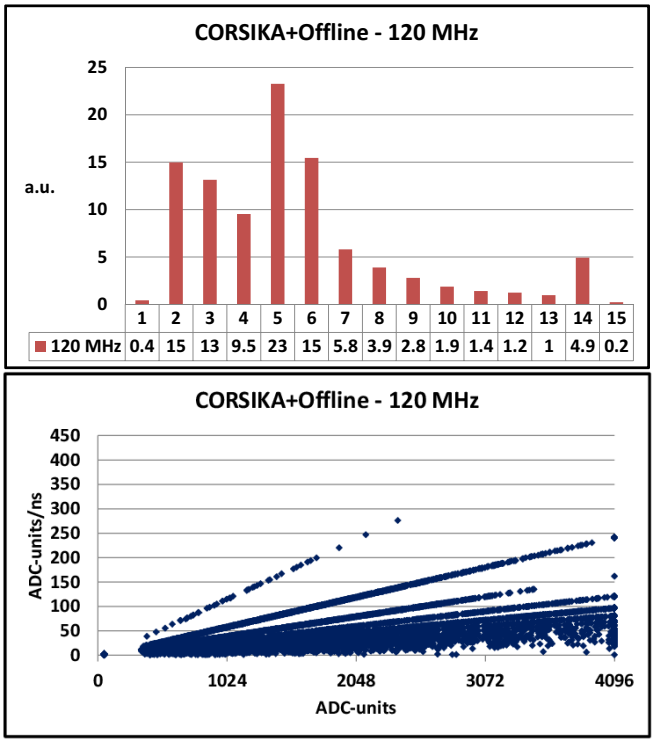


Fig. 6. A histogram showing a contribution of rise times for 1-,2- and more time bins for CORSIKA + Offline simulations with 120 MHz sampling frequency (upper graph) as well as a slope distribution of rising edges of signal waveforms vs. an amplitudes for 120 MSps (lower graph). Branches correspond to 1-, 2- and more time bins slopes from a pedestal level to maximum a maximum value.

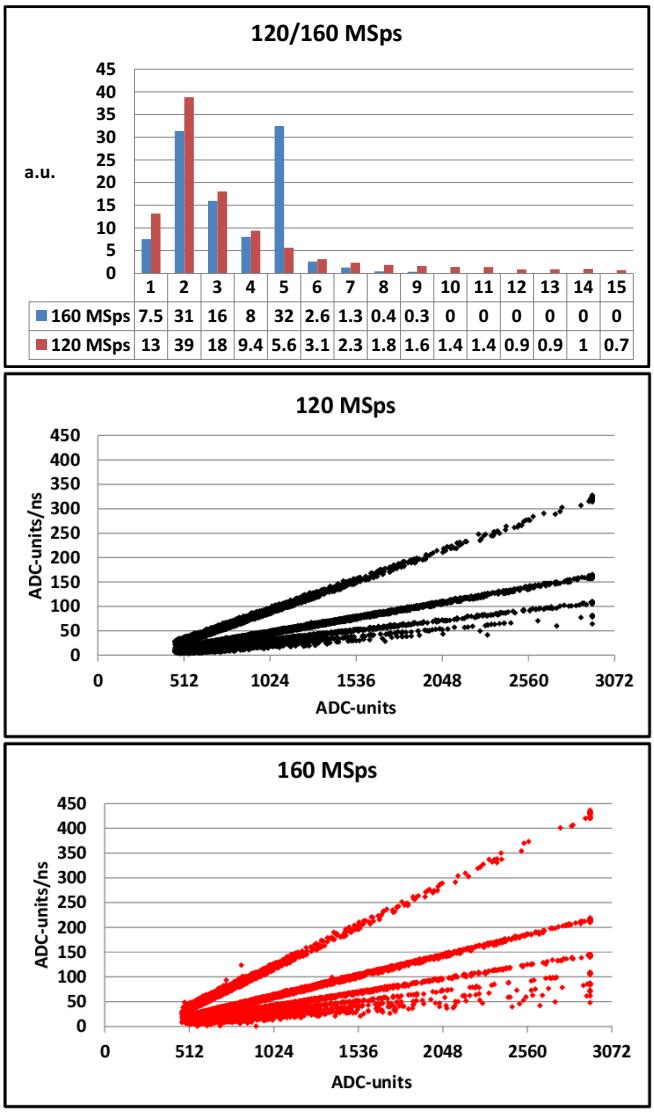


Fig. 7. A histogram showing a contribution of rise times for 1-,2- and more time bins for real measurements with 120 and 160 MSps (upper graph) as well as a slope distribution of rising edges of signal waveforms vs. an amplitudes for 120 MSps (middle graph) and 160 MSps (lower graph). Branches correspond to 1-, 2- and more time bins slopes from a pedestal level to a maximum value.

negligible (∼0.4%). Real measurements without anti-aliasing filters give much bigger 1-time-bin contribution: 13% for 120 MSps and 7.5% for 160 MSps (Fig. 7a).

Fig. 6b and Fig. 7b show slope distributions for simulations and real measurements, respectively, both for 120 MHz sampling frequency. We see that anti-aliasing filter introduces a significant inclination of the signal rising edges, which may dramatically affect a timing analysis based on rising times distributions and important for e.g. splitting of muon "pancakes" generated in very inclined showers. Charged muons are deflected in the Earth magnetic field and create two sub-showers. A precise timing analysis allows a significant improvement of a geometrical shower reconstruction.

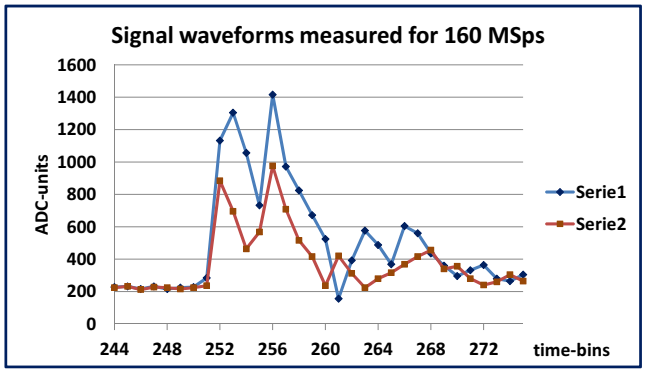


Fig. 8. Samples of signal waveforms registered with 160 MSps, which manifest light reflections from the Tyvec® walls.

Fig. 7c shows that for the 160 MSps a contribution signal waveforms with 1-time-bin rising edges is still high. It means a real rise time of many signal from the pedestal level to the maximal value may be even shorten than an interval of a single time bin.

Rising times for 160 MSps reach even ∼440 ADC-units/ns, which is 2-3 times faster than with even 5-pole Bessel filter. This may suggest that the rising edge is in fact steeper and with

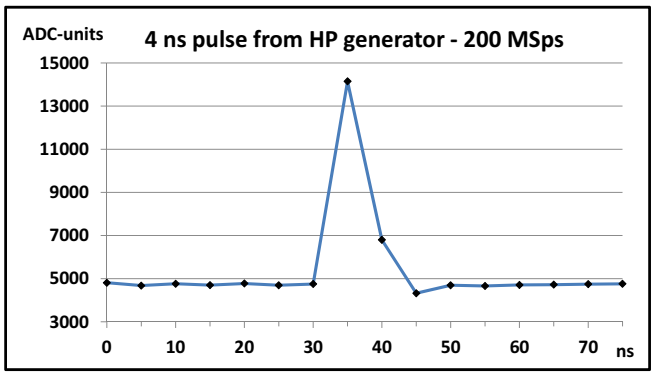


Fig. 9. A signal waveform for 4 ns pulse from the HP generator for the sampling frequency 200 MHz.

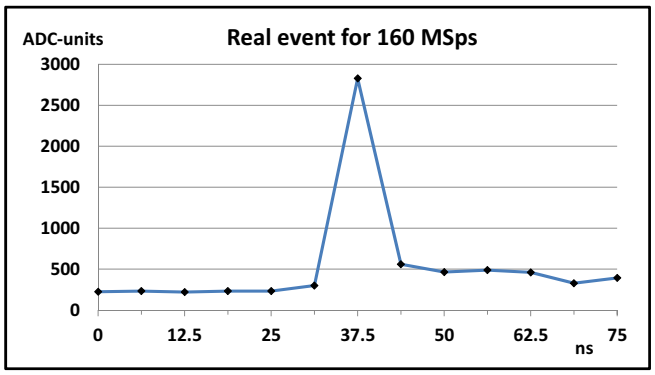


Fig. 10. A signal waveform of a real very short pulse registered for 160 MSps.

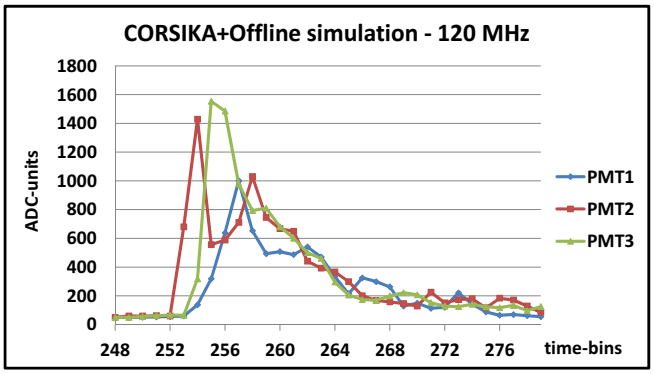


Fig. 11. Samples of signal waveforms simulated by the CORSIKA and Offline packages with 120 MSps, which manifest light reflections from the Tyvec® walls.

a faster sampling frequencies we would get still non-negligible amount of events located on the 1-time-bin branch.

A significant contribution of events with 5-time-bin rising edge comes from a light reflections from a Tyvec® walls (see samples of measured signal waveforms on Fig. 8 and simulated on Fig. 11). 3-4 time-bins for 160 MSps correspond to 18.75 - 25 ns and to 4 - 5 m of an additional geometrical distance for a light by n = 1.333 for a pure water.

The Front-End Board with Cyclone® V E is able to register even a 1-time-bin very short pulse. Fig. 9 shows a very short 4 ns pulse registered in the lab for a signal provided from the HP generator. ADC was working with 200 MHz sampling frequency. A similar pulse (Fig. 10) has been registered in real conditions for a signal obtained from PMTs of the tested surface detector. If the Front-End Board had been equipped in the anti-aliasing filter such pulses would have been strongly suppressed and probably not registered due to too low amplitude below a detection threshold.

## VI. DCT TRIGGER CONFIGURATIONS

16-point DCT algorithm for 120, 160 or 200 MHz sampling frequencies corresponds to 125, 93.75 or 75 ns, respectively, of sliding windows. We are interested in signal waveforms with a jump from a pedestal level to a maximum value and with the exponentially attenuated tails. As a pattern we can select 2, 3 or more time bins (Fig. 12) on a pedestal level following by the jump. DCT coefficients significantly depend on an amount of initial (pedestal level) time bins (Fig. 13).

The DCT coefficients are scaled to the $1^{st}$ harmonics. For the variant of 4 time bins, the DCT[1] is sometimes (for a particular tail slope $\alpha$ = 0.16667) very close to zero and as denominator in a scaling arbitrary units (a.u.) gives a huge value of a fraction (Fig. 14). So, the 4 time-bin variant provides an almost negligible sensitivity for $\alpha \neq 0.16667$.

For 160 and 200 MHz sampling frequencies 3 time-bins variants manifest the same undesirable coefficient characteristics similar to shown on Fig. 13c due to an almost singularity because of DCT[1]. for final test we select 3 time-bin variant

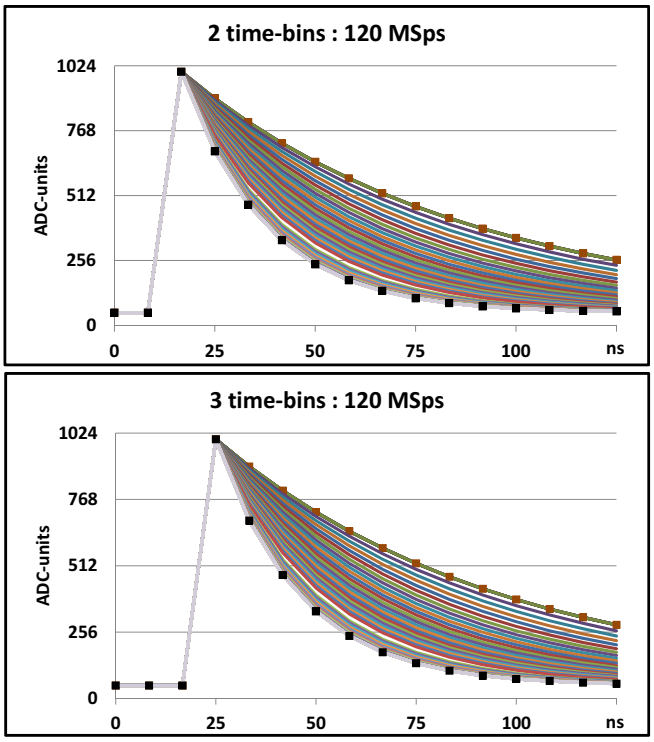


Fig. 12. Shapes of signal waveforms (for 120 MSps) giving the DCT trigger. The upper graph corresponds to an analysis of a signal waveform, where a jump appears on the $2^{nd}$ time-bin, the lower one for the $3^{rd}$ one.

for 120 MSps and 2 time-bin variants for 160 and 200 MSps, respectively.

DCT coefficients are preliminary calculated in an external C program for various $\alpha$ slopes. They are stored in the FPGA ROM and multiplexed in real time to keep arbitrary selected DCT rate ($\sim$6 Hz). In order to provide a sufficient calculation precision with a reasonably resources occupancy the DCT coefficients for ROM are selected as 12-bit fixed-point data.

For 160 and 200 MSps the DCT[8]/DCT[1] is almost independent of the tail slopes and are almost zeroed. We will neglect this coefficients as almost insensitive on signal waveform shapes.

The AHDL code for the FPGA contains a sigma-delta algorithm multiplexing several variants of bordering slopes to keep the stable DCT trigger rate in huge daily temperature variation [14]. This algorithm has been already successfully tested in Nov. 2014

## VII. CONCLUSIONS

We planned to deploy 7 Front-End Boards in a hexagon of the surface detectors in the Pierre Auger Engineering Array. As we see from Fig. 13 and Fig. 14 a configuration with 4 time-bins on a pedestal level is not suitable for a detection. A scaling fails due to a small DCT[1] coefficient for 15th k index. The variant with 3 time bins seems to be more appropriate, although 2 time bin variant also was tested in 2014 and passed successfully tests on the FEB with Cyclone III.

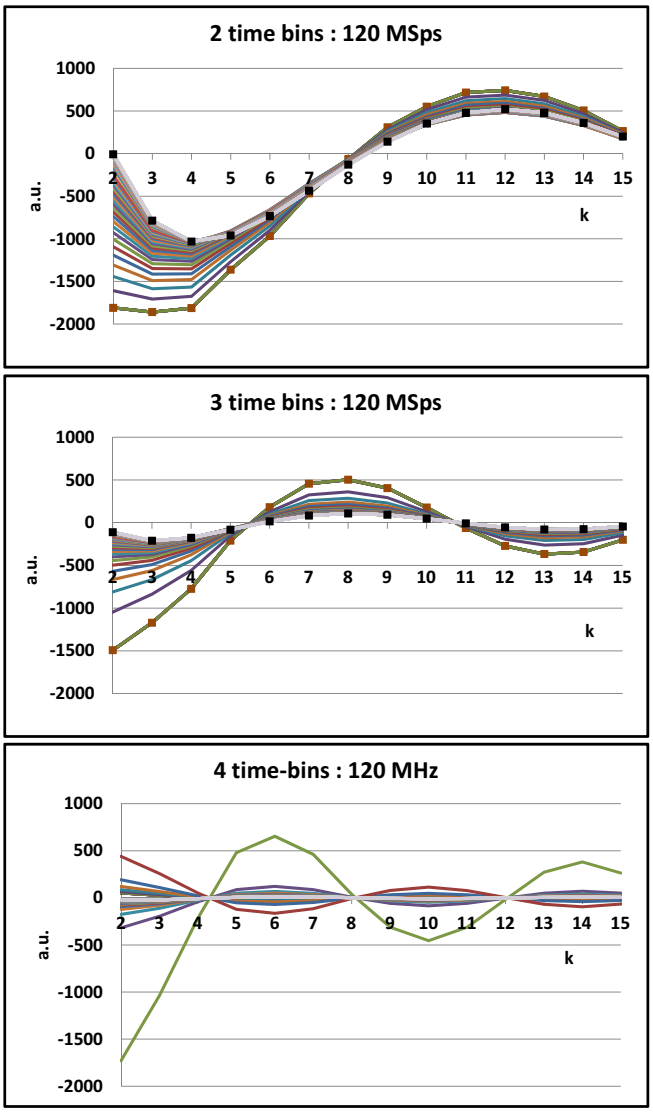


Fig. 13. DCT coefficients (for 120 MSps) giving the DCT trigger. The upper graph corresponds to an analysis of a signal waveform, where a jump appears on the $2^{nd}$ time-bin, the middle one for the $3^{rd}$ one and the lower graph for the $4^{th}$ one.

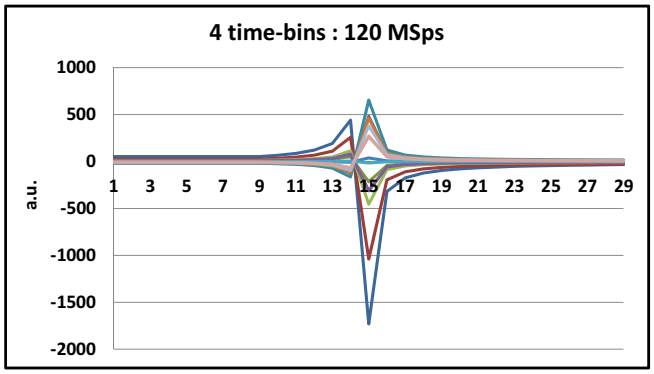


Fig. 14. DCT coefficients (for 120 MSps) vs. index of the tail slope. For k=15 the DCT[1] is close to zero (as denominator in a scaling) and DCT[k]/DCT[1] become huge values in comparison the other scaled DCT cofficients.

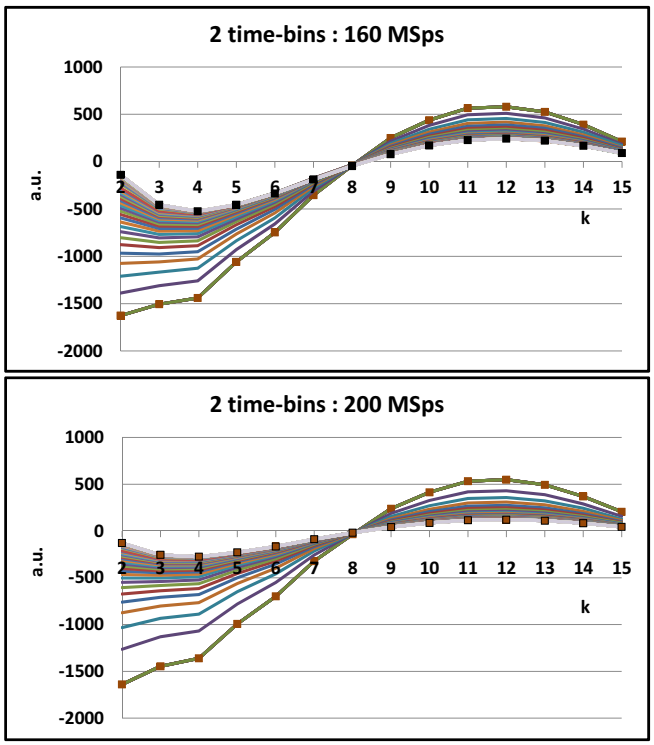


Fig. 15. DCT coefficients for 160 and 200 MSps giving the DCT trigger.

## ACKNOWLEDGMENT

This work was supported by the National Science Centre (Poland) under NCN Grant No. 2013/08/M/ST9/00322

## REFERENCES

[1] J. Abraham et al., [Pierre Auger Collaboration], "Properties and Performance of the Prototype Instrument for the Pierre Auger Observatory", *Nucl. Instr. Meth.*, ser. A, vol. 523, pp. 50-95, May 2004. DOI: 10.1016/j.nima.2003.12.012

[2] P. Abreu et al.,[ Pierre Auger Collaboration], "The exposure of the hybrid detector of the Pierre Auger Observatory", *Astroparticle Phys.* vol. 34 Issue: 6 pp. 368-381, Jan. 2011. DOI: 10.1016/j.astropartphys.2010.10.001

[3] M. Settimo et al.,[ Pierre Auger Collaboration], "Measurement of the cosmic ray energy spectrum using hybrid events of the Pierre Auger Observatory", *European Phys. Journal Plus* vol. 127 Issue: 8 Article Number: 87, 15 pages, Aug 2012. DOI: 10.1140/epjp/i2012-12087-9

[4] J. Abraham et al., [Pierre Auger Collaboration], "Trigger and aperture of the surface detector array of the Pierre Auger Observatory", *Nucl. Instr. Meth.*, ser. A, vol. 613, pp. 29-39, Jan. 2010. DOI: 10.1016/j.nima.2009.11.018

[5] P. Abreu et al.,[ Pierre Auger Collaboration], "Search for ultrahigh energy neutrinos in highly inclined events at the Pierre Auger Observatory", *Phys. Rev. D* vol. 84 Issue: 12, No: 122005, Dec. 2011. DOI: 10.1103/PhysRevD.84.122005

[6] P. Abreu et al.,[ Pierre Auger Collaboration], "Search for point-like sources of ultra-high energy neutrinos at the Pierre Auger Observatory and improved limit on the diffuse flux of tau neutrinos", *Astrophys. Journal Lett.* vol. 755 Issue: 1 Article Number: L4 7 pages, Aug. 2012. DOI: 10.1088/2041-8205/755/1/L4

[7] Z. Szadkowski, K. Pytel, *Artificial neural network as a FPGA trigger for a detection of very inclined "young" showers*, IEEE Trans. on Nucl.

Science, vol. 63, Issue 3, pp. 1002-1009, June 2015.
DOI: 10.1109/TNS.2015.2421412

[8] Z. Szadkowski, "A spectral $1^{st}$ level FPGA trigger for detection of very inclined showers based on a 16-point Discrete Cosine Transform for the Pierre Auger Observatory", *Nucl. Instr. Meth.*, ser. A, vol. 606, pp. 330-343, July 2009.
DOI: 10.1016/j.nima.2009.03.255

[9] Z. Szadkowski, "Trigger Board for the Auger Surface Detector with 100 MHz Sampling and Discrete Cosine Transform", *IEEE Trans. on Nucl. Science*, vol. 58, pp. 1692-1700, Aug. 2011.
DOI: 10.1109/TNS.2011.2115252

[10] Z. Szadkowski "An optimization of 16-point Discrete Cosine Transform Implemented into a FPGA as a Design for a Spectral First Level Surface Detector Trigger in Extensive Air Shower Experiments", (2011) *Applications of Digital Signal Processing*, InTech, ISBN 978-953-307-406-1, Croatia.

[11] Z. Szadkowski, "Optimization of the detection of very inclined showers using a spectral DCT trigger in arrays of surface detectors", *IEEE Trans. on Nucl. Science*, vol. 60, no 5, pp. 3647-3653, Oct. 2013.
DOI: 10.1109/TNS.2013.2280639

[12] Z. Szadkowski, "The concept of an ACEX® cost-effective first level surface detector trigger in the Pierre Auger Observatory", *Nucl. Instr. Meth.*, ser. A, vol 551, pp. 477-486, Oct. 2005.
DOI: 10.1016/j.nima.2005.06.049

[13] Z. Szadkowski, K.-H. Becker, K.-H. Kampert, "Development of a new first level trigger for surface array in the Pierre Auger Observatory based on the Cyclone™ Altera® FPGA", *Nucl. Instr. Meth.*, ser. A, vol. 545, pp. 793-802, June 2005.
DOI: 10.1016/j.nima.2005.03.118

[14] J. Abraham et al., [Pierre Auger Collaboration], "Atmospheric effects on extensive air showers observed with the surface detector of the Pierre Auger Observatory", *Astroparticle Phys.* vol. 32 Issue: 2 pp. 89-99, Sept. 2009.
DOI: 10.1016/j.astropartphys.2009.06.004